FLUID FREE SURFACE PROXIMITY EFFECT ON A SPHERE VERTICALLY ACCELERATED FROM REST

Department of the Navy, Naval Ordnance Systems Command Weapon Dynamics Division
Contract N600(19)59368 to the California Institute of Technology and Task Assignment Number RRRE-04001/216-1/R009-01-01 to the U.S. Naval Ordnance Test Station, Pasadena

HYDRODYNAMICS LABORATORY
KÁRMÁN LABORATORY OF FLUID MECHANICS AND JET PROPULSION
CALIFORNIA INSTITUTE OF TECHNOLOGY
PASADENA, CALIFORNIA

Hydrodynamics Laboratory
Kármán Laboratory of Fluid Mechanics and Jet Propulsion
California Institute of Technology
Pasadena, California

FLUID FREE SURFACE PROXIMITY EFFECT ON A SPHERE VERTICALLY ACCELERATED FROM REST

Department of the Navy, Naval Ordnance Systems Command Weapon Dynamics Division
Contract N600(19)59368 to the California Institute of Technology and Task Assignment Number RRRE-04001/216-1/R009-01-01 to the U.S. Naval Ordnance Test Station, Pasadena

J. G. Waugh
and
A. T. Ellis

Report No. E-124.2 June 1967

ABSTRACT

Theory is developed to estimate the effect of free surface proximity on the initial added mass of a sphere accelerated vertically upward from rest in an ideal fluid. It is assumed that the acceleration regime is sufficiently brief that inertial forces predominate and gravitational effects may be neglected. Results of tests in water indicate that while there are slight viscous and gravitational effects over the acceleration regime, the agreement between theory and experiment is good. It is concluded that over briefer acceleration regimes these effects would decrease and the agreement would improve.

FLUID FREE SURFACE PROXIMITY EFFECT ON A SPHERE VERTICALLY ACCELERATED FROM REST

J. G. Waugh and A. T. Ellis

1. Introduction

This report comprises the final technical report on work supported by the Department of the Navy, Bureau of Naval Weapons (and subsequently the Naval Ordnance Systems Command) on Contract N600(19)59368 to the California Institute of Technology, and Task Assignment No. RRRE-04001/216-1/R009-01-01 to the U. S. Naval Ordnance Test Station, Pasadena, California. One previous technical report was issued (Ref. 1) and three papers were published in the open literature (Refs. 2-4).

A major problem in the design of bodies moving through a fluid is the evaluation of the inertial resistance of the fluid when the body is accelerated. This inertial resistance affects the motion of the body and is usually described in terms of an apparent increase in the mass (added mass) of the body (Ref. 5). Although in theory added masses can be computed for any flow situation and used to determine a complete expression for the ideal pressure forces, the actual solution of the problem often proves mathematically intractable. The greatest difficulties are found in the determination of motion of bodies not deeply submerged; that is, bodies close to a free surface. In this category are weapons of primary importance to national defense, such as aircraft torpedoes, other air-to-water missiles, and water-to-air missiles such as POLARIS and SUBROC. The importance of added mass in service missile technology is evidenced by the fact that these missiles experience perturbations in passing through the water-air interface which pose problems in their subsequent operation, and which can in part be ascribed to added mass effects.

Despite the importance of water-exit perturbations in missile behavior and the large effect that added mass must have in these perturbations, there appears to be little information of a basic nature. It is known that potential frictionless flow exists in a real fluid during the first instant after a body is accelerated from rest (Ref. 6). Generally speaking, resistance to acceleration from rest in a real fluid should agree with ideal fluid theory and quite good agreement has been obtained for a sphere when all solid boundaries are remote (Ref. 5), but there do not appear to be any tests of this hypothesis for a body in the presence of a free surface. This suggests the possibility of developing theory for a body of mathematically tractable shape in the presence of a free surface and correlating this theory with experimental results obtained during the first instant after this body has been accelerated from rest. It was decided to conduct theoretical and experimental studies on the initial added mass of a sphere accelerated vertically upward from rest at varied depths below a free fluid surface. These studies are described in this report.

2. Theory

In the following theoretical discussion we assume an ideal fluid with orthogonal coordinate axes x, y, z such that the x, z-plane lies in the undisturbed free fluid surface and the y-axis is directed positively vertically upward (Fig. 1). Let the velocity potential which satisfies all boundary conditions be $\phi(x, y, z, t)$, the fluid velocity (assumed to be small everywhere) be $v = -\nabla\phi$, and all disturbances arising from ϕ be negligible at a great distance. Then the pressure equation for time-dependent irrotational flow is

$$\frac{p}{\rho} + \frac{1}{2}(\phi_x^2 + \phi_y^2 + \phi_z^2) + gy - \frac{\partial\phi}{\partial t} = C(t) \qquad (1)$$

where $C(t)$ is an arbitrary function of time. If $\eta = \eta(x, z, t)$ is the height of the free surface (assumed to be small) measured from the plane $y = 0$, the linearized formula for surface deformation may be obtained from the following considerations. The velocity components

ϕ_x, ϕ_y, ϕ_z must be small at the surface, and therefore the quadratic terms $\phi_x^{\,2}$, $\phi_y^{\,2}$, $\phi_z^{\,2}$ may be dropped from Eq. (1). Furthermore p is constant at the free surface. Then Eq. (1) becomes

$$\frac{p}{\rho} + g\eta - \frac{\partial\phi}{\partial t} = C(t) \tag{2}$$

If C(t) and the additive constant, p/ρ , are supposed merged in the value of $\partial\phi/\partial t$, Eq. (2) becomes

$$g\eta = \left(\frac{\partial\phi}{\partial t}\right)_{y=\eta} \approx \left(\frac{\partial\phi}{\partial t}\right)_{y=0} \tag{3}$$

At the free surface, the velocity of each fluid particle in the surface must be tangential to the surface. Expressing the equation of the free surface as an implicit function

$$F(x, y, z, t) \equiv y - \eta(x, z, t) = 0 \tag{4}$$

this kinematic condition is given by

$$\frac{dF}{dt} = 0 \tag{5}$$

From Eqs. (4) and (5)

$$-\frac{\partial\eta}{\partial t} + \frac{\partial\phi}{\partial x}\frac{\partial\eta}{\partial x} + \frac{\partial\phi}{\partial z}\frac{\partial\eta}{\partial z} - \frac{\partial\phi}{\partial y} = 0 \tag{6}$$

Neglecting the product terms in Eq. (6)

$$\frac{\partial\eta}{\partial t} + \frac{\partial\phi}{\partial y} = 0 \qquad (y = 0) \tag{7}$$

which states that the surface deformation velocity, $\partial\eta/\partial t$, must be equal to the surface perturbation velocity, $-\partial\phi/\partial y$, evaluated in the plane $y = 0$. The pressure condition on ϕ from Eq. (3), and the kinematic condition from Eq. (7), can be combined as follows

$$\frac{\partial}{\partial t}\left(\frac{1}{g}\,\frac{\partial\phi}{\partial t}\right) = \frac{\partial\eta}{\partial t} = -\,\frac{\partial\phi}{\partial y} \tag{8}$$

or

$$\frac{\partial^2\phi}{\partial t^2} + g\,\frac{\partial\phi}{\partial y} = 0 \qquad (y = 0) \tag{9}$$

Now consider a disturbance generated in the fluid involving high fluid accelerations, but considered over a sufficiently brief interval of time that fluid displacements and velocities are small. Then the gravitational effect will be negligible and inertial forces will predominate. Under these assumptions, the term $g\,(\partial\phi/\partial y)$ may be dropped in Eq. (9) to yield

$$\frac{\partial^2\phi}{\partial t^2} = 0 \qquad (y = 0) \tag{10}$$

and neglecting g (i.e., setting $g = 0$) in Eq. (3) implies

$$\frac{\partial\phi}{\partial t} = 0 \qquad (y = 0) \tag{11}$$

We may satisfy the conditions of Eq. (10) and (11) by constructing $\phi\,(x, y, z, t)$ to be independent of t in $y = 0$. Thus if we assume ϕ_o is the velocity potential in the absence of the surface, we can construct ϕ by writing

$$\phi = \phi_o(x, y, z, t) + \phi_1(x, y, z, t) \tag{12}$$

where ϕ_1 is a potential function which corrects ϕ_o for the presence of the fluid surface. In view of the above conditions, it suffices to take

$$\phi_1(x, o, z, t) = -\,\phi_o(x, o, z, t) \tag{13}$$

If the disturbance is caused by a moving body in the fluid, we may assume a function ϕ_2 which will correct Eq. (12) to satisfy the boundary condition on the body. That is,

$$\phi = \phi_o(x, y, z, t) + \phi_1(x, y, z, t) + \phi_2(x, y, z, t) \tag{14}$$

satisfies the body boundary condition. Assuming a function ϕ_3 Eq. (14) may be corrected for the presence of the fluid surface, etc. In this way we can construct a sequence of potential functions ϕ_i such that

$$\phi(x, y, z, t) = \phi_o(x, y, z, t) + \sum_{i=1}^{\infty} \phi_i(x, y, z, t) \tag{15}$$

satisfies the fluid surface and boundary conditions. If, in addition, the body has a mathematically tractable shape such as a sphere, and experimental conditions approximate those assumed in the theory, a correlation between theory and experimental data may be obtained.

We consider, then, a sphere accelerated vertically upward from rest at different depths below the fluid surface. Referring to Fig. 1, the potential function for a sphere of radius, a, in fluid of infinite extent, moving upward along the y-axis is

$$\phi_o = \frac{U(t)\,a^3}{2} \frac{\cos\theta}{r_o^2} = \frac{U(t)\,a^3}{2} \frac{y + h_o(t)}{r_o^3} \tag{16}$$

where $U(t)$ is the sphere velocity and $h_o(t)$ is the instantaneous position of the center of the sphere below the origin. Equation (16) is the velocity potential of a doublet with its axis directed along positive y and strength $U(t)\,a^3/2$. The boundary condition on the sphere is given by

$$- \frac{\partial \phi_o}{\partial r_o} = U(t) \cos \theta , \qquad (r_o = a) \tag{17}$$

From the preceding theory, through the use of successive "image" doublets in the sphere and free surface the desired velocity potential may be obtained.

If we denote the doublet strengths in the primary sphere by $\mu_{s\nu}$ and those in the free surface by $\mu_{i\nu}$, we obtain for the doublet strengths and locations

$$\mu_{so} = \mu_{io} = \frac{U(t)\, a^3}{2} \tag{18}$$

$$\mu_{s\nu} = \mu_{i\nu} = \frac{U(t)\, a^3}{2} \prod_{p=1}^{\nu} (-1)^{\nu} \left(\frac{a}{h_o + h_{p-1}} \right)^3 ,$$

$$(\nu = 1, 2, 3, \ldots) \tag{19}$$

where

$$h_p = h_o - \frac{a^2}{h_o + h_{p-1}} , \quad (p = 1, 2, 3, \ldots) \tag{20}$$

The primary sphere image doublet vertical positions, $y_{s\nu}$, are given by $- y_{s\nu} = h_\nu$ and the surface image vertical positions, $y_{i\nu}$, by $y_{i\nu} = h_\nu$. The limit points for the sphere and surface image doublet positions are derived in the Appendix. Note that $- y_{so} = h_o = y_{io}$. Then the desired velocity potential is given by

$$\phi = \frac{U(t)\, a^3}{2} \, G \tag{21}$$

where

$$G = \frac{y + h_o}{r_o^3} + \sum_{\nu=1}^{\infty} (-1)^{\nu} \prod_{p=1}^{\nu} \left(\frac{a}{h_o + h_{p-1}} \right)^3 \left(\frac{y + h_\nu}{r_\nu^3} \right)$$

$$+ \frac{y - h_o}{s_o^3} + \sum_{\nu=1}^{\infty} (-1)^{\nu} \prod_{p=1}^{\nu} \left(\frac{a}{h_o + h_{p-1}} \right)^3 \left(\frac{y - h_\nu}{s_\nu^3} \right) \qquad (22)$$

and

$$r_\nu^2 = R^2 + (y + h_\nu)^2 \qquad (\nu = 0, 1, 2, \ldots) \qquad (23)$$

$$s_\nu^2 = R^2 + (y - h_\nu)^2 \qquad (\nu = 0, 1, 2, \ldots) \qquad (24)$$

It should be noted that the h_p as well as h_o are functions of t. This is not shown explicitly in Eq. (19), (20), and (22) to avoid complication.

Differentiating Eq. (21) with respect to time,

$$\frac{\partial \phi}{\partial t} = \frac{\dot{U}(t)\, a^3}{2} G + \frac{U(t)\, a^3}{2} \frac{\partial G}{\partial t} \qquad (25)$$

The terms of $\partial G/\partial t$ contain factors of the order of $U(t)$ which decrease and vanish as $U(t) \longrightarrow 0$. It can be shown that $\partial G/\partial t$ converges for finite $U(t)$ and vanishes for $U(t) = 0$. Under the assumption that $U(t)$ is small over the time interval considered, Eq. (25) becomes

$$\frac{\partial \phi}{\partial t} = \frac{\dot{U}(t)\, a^3}{2} G \qquad (26)$$

The pressure on the sphere is given by

$$p = \rho \left(\frac{\partial \phi}{\partial t} - gy - \frac{|v^2|}{2} \right) \tag{27}$$

The term gy in Eq. (27) on integration over the sphere gives the hydrostatic or buoyancy force. This does not contribute to the fluid resistance and will be neglected. Experimentally, this force can be eliminated by making the sphere neutrally buoyant. The velocity $|\vec{v}|$ is of the order of U(t) and hence the quadratic term $|v^2|$ will be neglected. From Eq. (26) and (27), and integrating the pressure, p, over the sphere surface, we obtain for the force, F, arising from fluid resistance on the sphere,

$$F = -2\pi a^2 \int_0^{\pi} p \sin\theta \cos\theta \, d\theta$$

$$= -\dot{U}(t) \left[\pi a^5 \rho \int_0^{\pi} G \sin\theta \cos\theta \, d\theta \right] \tag{28}$$

This may be written

$$K_o = \frac{F}{-\frac{4}{3}\pi a^3 \rho \dot{U}(t)} = \frac{3}{4} a^2 \int_0^{\pi} G \sin\theta \cos\theta \, d\theta \tag{29}$$

where K_o, the added mass coefficient, is the initial apparent increase in the mass of the sphere on acceleration from rest neglecting gravitation effects (g = 0), expressed in terms of the mass of fluid displaced by the sphere. In order to compute the added mass coefficients it is convenient to introduce the terms

$b_{s\nu}$ = distance of the νth doublet within the sphere from the primary sphere doublet

$b_{i\nu}$ = distance of the νth free surface image doublet from the primary sphere doublet

Then

$$b_{s\nu} = \frac{a^2}{h_o + h_{\nu-1}} \tag{30}$$

$$b_{i\nu} = 2h_o - \frac{a^2}{h_o + h_{\nu-1}} = 2h_o - b_{s\nu} \tag{31}$$

The following expansions of the image doublets in terms of the primary sphere coordinates are obtained from surface zonal harmonic theory (Ref. 7)

$$\frac{y + h_\nu}{r_\nu^3} = \frac{\cos\theta_{s\nu}}{r_\nu^2} = \frac{1}{r_o^2} P_1(\cos\theta) + \frac{2b_{s\nu}}{r_o^3} P_2(\cos\theta)$$

$$+ \frac{3b_{s\nu}^2}{r_o^4} P_3(\cos\theta) + \dots, \quad (r_o > b_{s\nu}) \tag{32}$$

$$\frac{y - h_\nu}{s_\nu^3} = \frac{\cos\theta_{i\nu}}{s_\nu^2} = -\left[\frac{1}{b_{i\nu}^2} + \frac{2r_o P_1(\cos\theta)}{b_{i\nu}^3}\right.$$

$$\left. + \frac{3r_o^2 P_2(\cos\theta)}{b_{i\nu}^4} + \dots\right], \quad (r_o < b_{i\nu}) \tag{33}$$

We now define the non-dimensionalized doublet positions

$$h'_\nu = \frac{h_\nu}{a}\,, \qquad (\nu = 0, 1, 2, \ldots) \tag{34}$$

From Eqs. (20), (30), (31), and (34)

$$\left.\begin{aligned} h'_\nu &= h'_o - \frac{1}{h'_o + h'_{\nu-1}} \\ b'_{s\nu} &= \frac{1}{h'_o + h'_{\nu-1}} \\ b'_{i\nu} &= 2h'_o - \frac{1}{h'_o + h'_{\nu-1}} = 2h'_o - b'_{s\nu} \end{aligned}\right\} (\nu = 1, 2, 3, \ldots) \tag{35}$$

Note that $b'_{so} = 0$ and $b'_{io} = 2h'_o$. To evaluate Eq. (29), we substitute Eq. (22) for G in the integrand. Making use of Eqs. (30) through (35) and the integral properties of surface zonal harmonics, integrals of the form

$$\left.\begin{aligned} a^2\int_0^\pi \frac{y + h_\nu}{r_\nu^3} \cos\theta \sin\theta \, d\theta &= \frac{2}{3}, \qquad (r_o = a,\ b'_{s\nu} < 1) \\ a^2\int_0^\pi \frac{y - h_\nu}{s_\nu^3} \cos\theta \sin\theta \, d\theta &= -\frac{4}{3b'^3_{i\nu}}, \qquad (r_o = a,\ b'_{i\nu} > 1) \end{aligned}\right\} \tag{36}$$

are obtained which apply to the sphere and surface image doublets, respectively. Substituting the values of the integrals, we obtain for the added mass coefficient

$$K_o = \frac{1}{2} + \frac{1}{2} \sum_{\nu=1}^{\infty} (-1)^{\nu} \prod_{p=1}^{\nu} b_{sp}^{'3} - \frac{1}{b_{io}^{'3}} - \sum_{\nu=1}^{\infty} (-1)^{\nu} \prod_{p=1}^{\nu} \frac{b_{sp}^{'3}}{b_{i\nu}^{'3}} \tag{37}$$

It can be shown that Eq. (37) converges for $1 \leq h_o' \leq \infty$, that is, for all depths of complete sphere submergence. At great depths, $h_o' = \infty$ and $K_o = 0.5$, the added mass coefficient of a sphere in fluid of infinite extent. At the least depth of complete sphere submergence where the sphere is tangent to the fluid surface, $h_o' = 1$ and the added mass coefficient becomes

$$K_o = \frac{3}{2} \sum_{\nu=1}^{\infty} \frac{(-1)^{\nu-1}}{\nu^3} - 1 = 0.35214\ldots \tag{38}$$

Values of K_o corresponding to various depths are given in Table 1 and K_o is shown plotted as a function of sphere depth in Fig. 2.

The preceding theory has been developed on the assumption that $g = 0$, i.e., only inertial forces are considered. If we set $g = \infty$, no surface deformation can take place and we have the case of a sphere moving vertically toward a rigid wall (Ref. 7) for which the added mass coefficient is given by

$$K_{\infty} = \frac{1}{2} + \frac{3}{2}\left(\frac{a}{2h_o}\right)^3 = \frac{1}{2} + \frac{3}{2}\left(\frac{1}{2h_o'}\right)^3 \tag{39}$$

where h_o is now the distance of the sphere center from the wall (fluid surface). The added mass coefficient is shown plotted as a function of sphere depth in Fig. 2. Note that $K_{\infty} > K_{o}$ for all depths, K_{∞} decreasing asymptotically and K_{o} increasing asymptotically to 0.5 as the depth becomes infinite. In experimental studies where sphere displacement and velocity are necessarily involved and $0 < g < \infty$, both viscous and gravitational effects would arise and experimentally obtained added mass coefficients, K, should be greater than the corresponding theoretical values K_{o}, and even greater than K_{∞} for sufficiently viscous liquids. Where a valid correction can be made for viscous effects, it seems reasonable to assume that $K_{o} < K < K_{\infty}$.

3. Experiment

A highly polished hollow steel sphere was used in these studies. It was 1.004 ± 0.0001 in. in diameter and weighted to 9.3055 gm. so that it was 0.6411 gm. negatively buoyant with respect to water at an ambient temperature of $20^{o}C$. The sphere was positioned below the center and on the axis of a horizontal electromagnetic coil and accelerated vertically upward by discharging a bank of heavy-duty capacitors through the coil. An Ignitron mercury switch in the circuit prevented current oscillation and limited the electromagnetic effect to a half-wave sinusoidal pulse. The duration of the pulse was about 4 ms. and sphere displacement over the pulse interval less than 3/16 in. By accelerating the sphere in water and in air under otherwise similar conditions, it was possible to determine the added mass of the sphere.

A diagram of the electromagnetic acceleration apparatus is shown in Fig. 3. For launchings in water, the coil was positioned above the water surface to avoid hydrodynamic interference effects and the sphere was positioned at a suitable operating distance below the coil by means of a suspending thread. Varying sphere depths below the water surface were obtained by adjusting the water level. Since the negative buoyancy of the sphere was negligible, it was not necessary to consider any stored energy in the thread in the impulse to the sphere. For calibration launchings in air, where this would not be the case and where estimation of the energy in the thread would be uncertain, the sphere was supported by a Lucite rod. Because of hydrodynamic interference, a supporting rod could not be used in the tests with water. Tests were conducted in the test section of a non-magnetic Lucite water tank (Ref. 2) whose walls were at least 9 inches distant from the sphere; therefore wall effects could be ignored. An optical technique (Ref. 3) was used to obtain sphere displacement-time data. A more complete description of the electromagnetic accelerating technique, together with the theory involved, is given in Ref. 1.

Experimental data for sphere depths of 1.0, 1.5 and 2.5 diameters below the water surface are given in Table 2. For sphere accelerations in water, if we equate the total impulse acting on the sphere to the momentum change, we obtain

$$\int_0^{T/2} (F_w - D - G_w)\, dt = \int_0^{T/2} d\left[(M + m)\, U_\infty\right]$$

$$= \left[(M + m)\, U_\infty\right]_{t=0}^{t=T/2} = (M + m)\, U_\infty(T/2) \qquad (40)$$

where

$t = 0$ = time at start of acceleration regime

$t = T/2$ = time at end of acceleration regime

F_w = magnetic propulsive force in water

D = viscous drag force due to wall shear stress

G_w = negative-buoyancy force in water

M = mass of sphere

m = added mass of sphere

$U_\infty(t)$ = velocity of sphere through water

For the sphere launched in air the impulse momentum relationship (the added mass is negligible) is

$$\int_0^{T/2} (F_a - G_a)\, dt = MU_a(T/2) \tag{41}$$

where

$U_a(t)$ = velocity of sphere in air

F_a = magnetic propulsive force in air

G_a = gravitational force on sphere

Defining the impulses by

$$I_a = \int_0^{T/2} F_a \, dt \tag{42}$$

and using Eqs. (40) and (41), the following relationship can be deduced:

$$\frac{m}{M} = \frac{1}{U_\infty(T/2)} \left[\frac{U_a(T/2) + \frac{I_{G_a}}{M}}{\frac{I_{F_a}}{I_{F_w}}} - \frac{I_D}{M} - \frac{I_{G_w}}{M} \right] - 1 \tag{43}$$

Now the magnetic propulsive force on the sphere is not only a function of time but also a function of sphere position. Since the acceleration of the sphere will be greater in air than in water, its displacement toward the coil for corresponding times during the pulse period will be greater and its impulse greater. This difference in impulse was estimated by measuring the sphere displacement-time records and numerically integrating the data, making use of electromagnetic theory given in Ref. 1. For the data presented in Table 2, the impulse ratio $I_{F_a}/I_{F_w} = 1.002$. The pulse duration, T/2, was about 4.02 ms. and $g = 386.1$ in. sec.$^{-2}$. For launchings in air, the sphere left the supporting rod 0.08 ms. after pulse initiation (Ref. 1), but the correction to the magnetic force impulse due to this was found to be negligible. Therefore $I_{G_a}/M = 1.52$ in. sec.$^{-1}$. Now $M = 9.3055$ gm. and $G_w = 0.6411$ gm. from which $I_{G_w} = 0.107$ in. sec.$^{-1}$.

In order to compute the drag impulse, I_D, we will assume that boundary-layer separation did not occur over the acceleration regime, and flow outside the boundary layer was potential or very nearly so. Later we will show that these assumptions are justified. Referring to Eq. (22), the principal contribution to the velocity potential is given by the primary sphere and first surface and sphere image doublets; the contributions of succeeding doublets diminish rapidly, especially at greater depths. We then assume the approximate velocity potential,

$$\phi = \frac{U(t)\,a^3}{2}\left[\frac{y+h_o}{r_o^3} + \frac{y-h_o}{s_o^3} - \left(\frac{a}{2h_o}\right)^3 \frac{y+h_1}{r_1^3}\right] \tag{44}$$

From Eqs. (32,), (33) and (44), we obtain the following approximate velocity potential in the neighborhood of the primary sphere

$$\phi = \frac{U(t)\,a^3}{2}\left[\frac{\cos\theta}{r_o^2} - \frac{1}{(2h_o)^2} - \frac{2r_o\cos\theta}{(2h_o)^3} - \left(\frac{a}{2h_o}\right)^3 \frac{\cos\theta}{r_o^2}\right] \tag{45}$$

By adding to Eq. (45) the velocity potential for a uniform stream, $U(t)$, in the negative y-direction, $\phi = U(t) r_o \cos\theta$, we obtain the approximate velocity potential for fluid flow outside the boundary layer

$$\phi = \frac{U(t)\,a^3}{2}\left[\frac{\cos\theta}{r_o^2} - \frac{1}{(2h_o)^2} - \frac{2r_o\cos\theta}{(2h_o)^3} - \left(\frac{a}{2h_o}\right)^3\frac{\cos\theta}{r_o^2}\right]$$

$$+ \; U(t)\, r_o \cos\theta \tag{46}$$

Then the fluid velocity outside the boundary layer over the sphere is given by

$$-\left(\frac{\partial\phi}{r_o\partial\theta}\right)_{r_o = a} = \frac{3U(t)}{2}\left[1 - \frac{1}{(2h_o')^3}\right]\sin\theta \tag{47}$$

Equation (47) indicates that depth has only a slight effect on the initial flow over the sphere on starting from rest. At great depth, Eq. (46) assumes the velocity potential of a sphere in uniform fluid flow of infinite extent. For unit velocity from Eq. (47),

$$U(\theta) = \frac{3}{2}\left[1 - \frac{1}{(2h_o')^3}\right]\sin\theta \tag{48}$$

From theory (Ref. 1 and 4), the drag impulse is given by

$$I_D = \frac{2\rho\sqrt{\frac{\nu}{\pi}}\int_0^{\pi} 2\pi\, a^2 \sin^2\theta\, U(\theta)\, d\theta \cdot U_\infty(T/2)\int_0^{T/2}\sqrt{\frac{T}{2}-\tau}\; e^{-2\alpha\tau}\sin^2\omega\tau\, d\tau}{\int_0^{T/2} e^{-2\alpha\tau}\sin^2\omega\tau\, d\tau} \tag{49}$$

where

ρ = density of water, 0.998 gm.cm.$^{-3}$ at 20°C

ν = kinematic viscosity of water, 1.007 x 10^{-2}cm.^{2}sec.$^{-1}$ at 20°C

α = damping constant of accelerating circuit, 1.955 x 10^2 rad.sec.$^{-1}$

ω = natural frequency of accelerating circuit, 7.789 x 10^2 rad.sec.$^{-1}$

a = radius of sphere, 0.502 in., 1.275 cm.

T/2 = pulse duration, 4.02 x 10^{-3}sec.

$U_\infty(T/2)$ = velocity of sphere in water at end of pulse regime, in.sec.$^{-1}$

The units of measurement have been mixed for convenience. In the laboratory the scale used for weighing was calibrated in grams and measurements of distances were made in inches.

Drag impulses for various sphere depths were calculated from Eq. (48) and Eq. (49) and the values of $U_\infty(T/2)$ given in Table 2. The right-hand integral in Eq. (49) was evaluated by Simpson's Rule and found to be 4.214 x 10^{-5}sec.$^{3/2}$. The other two integrals are easily evaluated, the left-hand integral in the numerator (considering only the integrand $\sin^3\theta$) having the value 4/3 and the integral in the denominator the value 9.670 x 10^{-4}sec.

The results show that $I_D = 5.28$, 5.23 and 5.25 gm. in. sec.$^{-1}$ for sphere depths of 2.5, 1.5 and 1.0 diameters respectively. Substituting these values and the values of $U_a(T/2)$ and $U_\infty(T/2)$ from Table 2 into Eq. (43) we obtain m/M, the added-mass-to-sphere-mass ratio. The mass of fluid displaced by the sphere is $M - G_w = 9.3055 - 0.6411 = 8.6644$ gm., and therefore $M/(M - G_w) = 1.0740$. Multiplying m/M by this factor we obtain $m/(M - G_w) = K$, the added mass coefficient.

For a comparison of theory and experiment to be valid, it is necessary to show that boundary-layer separation did not occur and fluid flow outside the boundary layer was essentially potential over the acceleration regime. The maximum (final) Reynolds number is 3.41×10^4, well below the critical (3×10^5), and laminar boundary-layer flow should obtain. E. Boltze showed (Ref. 6) that the distance a sphere launched impulsively from rest travels before separation starts is $S = 0.392$ a. H. Blasius (Ref. 6) showed in the case of two-dimensional flow that separation occurs at longer distances from the starting point for constant acceleration than for motion started impulsively. In brief, motion started impulsively appears to be the worst case. In these tests $a = 0.502$ in. and if the motion were started impulsively S would be 0.197 in. From data measurements, the displacement of the sphere during the force pulse was at most 0.188 in., and since its acceleration was a damped half-sine wave with respect to time, the sphere must have travelled some distance after pulse termination before separation began.

Added mass coefficients have been calculated from the data of Table 2 making use of the above theory. They are also presented in Table 2 together with fiducial limits corresponding to the 0.9546 and 0.9973 probability levels. These were calculated from statistical theory given in Ref. 1. Added mass coefficients obtained under similar conditions (Ref. 1) have been subsequently corrected for the drag impulse and their fiducial limits calculated. These data, given in Table 3, are slightly more accurate than those of Table 2, for they were obtained at a later time when more precise techniques for positioning the sphere with respect to the coil had been developed and electrical instrumentation for more accurately controlling launching conditions had been obtained. This probably accounts for the data of Table 2 being consistently below that of Table 3 and the low experimental value for a sphere depth of 2.5 diameters.

4. Discussion and Conclusions

The data of Tables 1 and 2 which are illustrated in Fig. 2 show good agreement between theory (K_o) and experiment. In no case did the experimental results and theory deviate significantly (0.9546 probability level), although the deviation for a depth of 2.5 sphere diameters is close to this level.

The data of Tables 1 and 3 show good agreement for sphere depths of 1/2 and 5/8 diameter, but deviate significantly (0.9546 probability level) for a depth of 1-1/8 diameters and highly significantly (0.9973 probability level) for depths of 3/4, 7/8, 1, 1-1/4, and 1-3/8 diameters.

From Fig. 2 it is seen that these significant deviations all lie above the theoretical curve for K_o and below the theoretical curve for K_∞, indicating that there may have been some gravitational effect during the acceleration regime. However, the good agreement between theory (K_o) and experiment from the standpoint of overall added mass coefficient values indicates that the theory provides a good approximation to the experimental initial added mass.

It is concluded that for briefer acceleration regimes, viscous and gravitational effects would decrease and the agreement between theory and experiment would improve.

Acknowledgment

The authors are indebted to Professor T. Y. Wu for reviewing the manuscript.

References

1. Mellsen, S. B., Ellis, A. T. and Waugh, J. G., "On the Added Mass of a Sphere in a Circular Cylinder Considering Real Fluid Effects," California Institute of Technology, Hydrodynamics Laboratory Report No. E-124.1, March 1966.

2. Waugh, J. G. and Ellis, A. T., "The Variable-Atmosphere Wave Tank," Cavitation Research Facilities and Techniques, A.S.M.E., 1964.

3. Waugh, J. G., Ellis, A. T., and Mellsen, S. B., "Techniques for Metric Photography," J. of the Society of Motion Picture and Television Engineers, Vol. 75, No. 1, January 1966.

4. Mellsen, S. B., Waugh, J. G., and Ellis, A. T., "Real Fluid Effects on an Accelerated Sphere Before Boundary-Layer Separation," A.S.M.E. Paper 66-WA/UNT-6, 1966.

5. Birkhoff, G., "Hydrodynamics," Princeton University Press, 1960, Chapter 6.

6. Schlichting, H., "Boundary Layer Theory," 4th Edition, McGraw-Hill, 1960, pp. 120, 185, 218-221.

7. Milne-Thomson, L. M., "Theoretical Hydrodynamics," Macmillan and Co., 1949, Chapter 16, pp. 437-447.

8. Khintchine, A. Y., "Continued Fractions," P. Noordhoff, Ltd., Groningen, The Netherlands, 1963, p. 15.

Nomenclature

a	-	radius of sphere
$b_{i\nu}$	-	distance of the νth free surface image doublet from the primary sphere doublet
$b_{s\nu}$	-	distance of the νth image doublet within the sphere from the primary sphere doublet
$C(t)$	-	arbitrary function of time
D	-	viscous drag force on sphere due to wall shear stress
F	-	fluid resistance on sphere due to inertial effects
F_a	-	magnetic propulsive force on sphere in air
F_w	-	magnetic propulsive force on sphere in water
g	-	gravitational acceleration
G_a	-	gravitational force on sphere
G_w	-	negative buoyancy force on sphere in water
h_ν	-	doublet vertical positions or distances from fluid surface. h_ν is negative for primary sphere and positive for surface image doublet positions. $(\nu = 0, 1, 2, \ldots)$
h_o	-	depth of primary sphere doublet
K	-	experimentally obtained initial added mass coefficient of a sphere accelerated from rest in water
K_o	-	initial added mass coefficient of a sphere accelerated vertically from rest in an ideal fluid under a free surface $(g = 0)$
K_∞	-	added mass coefficient of a sphere accelerated vertically in an ideal fluid under a free surface $(g = \infty)$
m	-	added mass of sphere
M	-	mass of sphere
p	-	fluid pressure

r_o - distance from primary sphere doublet

r_ν - distance from ν th primary sphere image doublet, $(\nu = 0, 1, 2, \ldots)$

R - distance from origin of a point in the fluid surface (x, z-plane)

s_ν - distance from ν th surface image doublet, $(\nu = 0, 1, 2, \ldots)$

t - time

T/2 - time duration of propulsive force pulse

$U(\theta)$ - potential fluid flow velocity over sphere for unit fluid velocity

$U_a(t)$ - velocity of sphere in air. $U_a(0) = 0$. $U_a(T/2)$ = velocity at end of propulsive force pulse.

$U_\infty(t)$ - velocity of sphere in water. $U_\infty(0) = 0$. $U_\infty(T/2)$ = velocity at end of propulsive force pulse.

$\vec{v}$ - fluid velocity. $\vec{v} = -\nabla\phi$

x, y, z - orthogonal fluid coordinate system. See Fig. 1.

α - damping constant of accelerating circuit

η - height of free surface measured from the plane of the undisturbed surface, i.e., from plane $y = 0$.

θ - angle between primary sphere radial coordinate, r_o, and vertical direction (y-axis). See Fig. 1.

$\theta_{s\nu}$ - angle between ν th primary sphere image doublet radial coordinate, r_ν, and vertical direction (y-axis). $(\nu = 1, 2, 3, \ldots)$

$\theta_{i\nu}$ - angle between ν th surface image doublet radial coordinate, s_ν, and vertical direction (y-axis). $(\nu = 0, 1, 2, \ldots)$.

$\mu_{s\nu}$ - strength of ν th primary sphere image doublet. $(\nu = 0, 1, 2, \ldots)$. μ_{so} = strength of primary sphere.

$\mu_{i\nu}$ - strength of ν th surface image doublet. $(\nu = 0, 1, 2, \ldots)$. $\mu_{i\nu} = \mu_{s\nu}$.

ν - kinematic viscosity of fluid

ρ - density of fluid

ϕ - velocity potential of fluid

ω - natural frequency of accelerating circuit

Note: A primed linear quantity indicates non-dimensionalization of that quantity by expressing it in terms of the sphere radius. Thus, $h_\nu' = h_\nu/a$.

Table 1

Theoretical Initial Added Mass Coefficient of a Sphere Accelerated Vertically From Rest Below an Ideal Fluid Surface (g = 0)

Initial Depth of Sphere Center (radii)	Added Mass Coefficient K_o
1	0.3521
1.1	0.3806
1.2	0.4038
1.3	0.4218
1.4	0.4360
1.5	0.4473
1.75	0.4661
2	0.4770
2.25	0.4837
2.5	0.4881
2.75	0.4910
3	0.4931
4	0.4970
5	0.4985
∞	0.5000

Table 2

Effect of Depth of Submergence on the Added Mass of a 1.004-Inch Diameter Sphere Accelerated Vertically Upward From Rest in Water

	Launchings in water			Launchings
Depth of sphere center below water surface (diameters)	2.5	1.5	1.0	in air
Sphere velocities just after acceleration regime (inches/second)	52.73	53.03	52.95	76.03
	52.53	51.80	53.29	75.75
	52.35	52.35	53.02	75.83
	51.99	52.29	52.85	75.16
	53.04	51.95	52.61	75.14
		52.18	53.23	75.49
Average sphere velocity just after acceleration regime (in/sec)	52.528	52.267	52.991	75.567
Average added mass coefficient (K)	0.487	0.495	0.474	
Average added mass coefficient (95.46 % limits)	0.475	0.483	0.465	
	0.499	0.507	0.482	
Average added mass coefficient (99.73 % limits)	0.469	0.477	0.461	
	0.506	0.513	0.486	

Table 3

Effect of Depth of Submergence on the Added Mass of a 1.004-Inch Diameter Sphere Accelerated Vertically Upward From Rest in Water*

Initial Depth of Sphere Center (diameters)	Average Added Mass Coefficient (K)	Fiducial Limits for Average Added Mass Coefficient 95.46%	99.73%
1/2	0.348	±0.009	±0.013
5/8	0.415	±0.006	±0.009
3/4	0.471	±0.015	±0.023
7/8	0.477	±0.006	±0.009
1	0.488	±0.006	±0.009
1-1/8	0.492	±0.006	±0.009
1-1/4	0.502	±0.007	±0.010
1-3/8	0.504	±0.005	±0.007

* The average added mass coefficients were obtained from six tests at each depth and were originally presented in Table 7 of Reference 1. They have subsequently been corrected for the drag impulse and their fiducial limits computed.

$$R^2 = x^2 + z^2$$
$$r_o^2 = R^2 + (y + h_o)^2$$

On sphere:

$$y + h_o = a \cos\theta$$
$$R = a \sin\theta$$

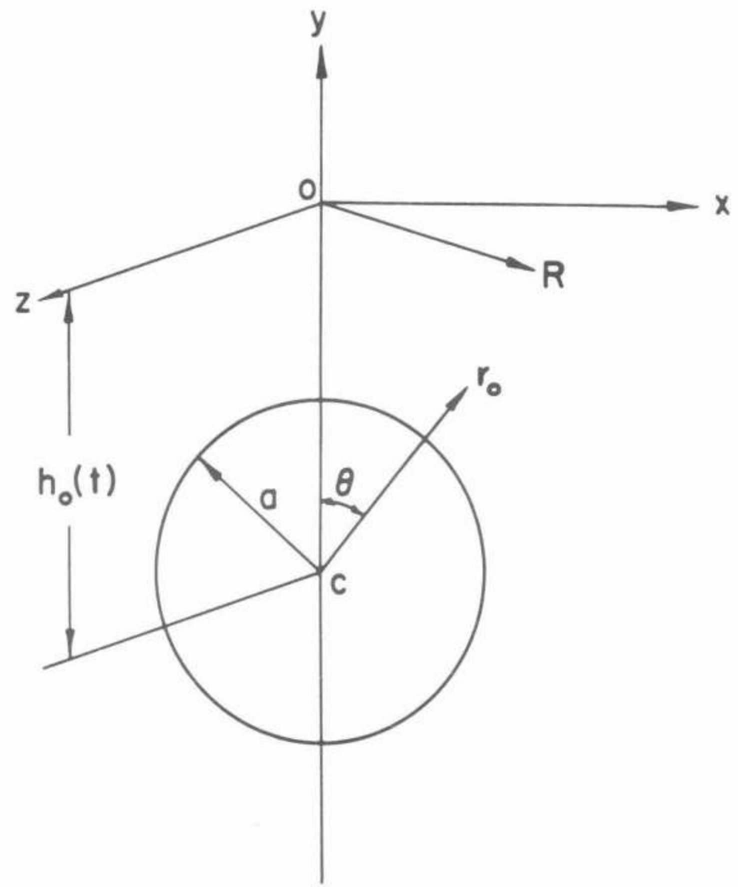

Figure 1 - Coordinate Systems for Fluid and Sphere

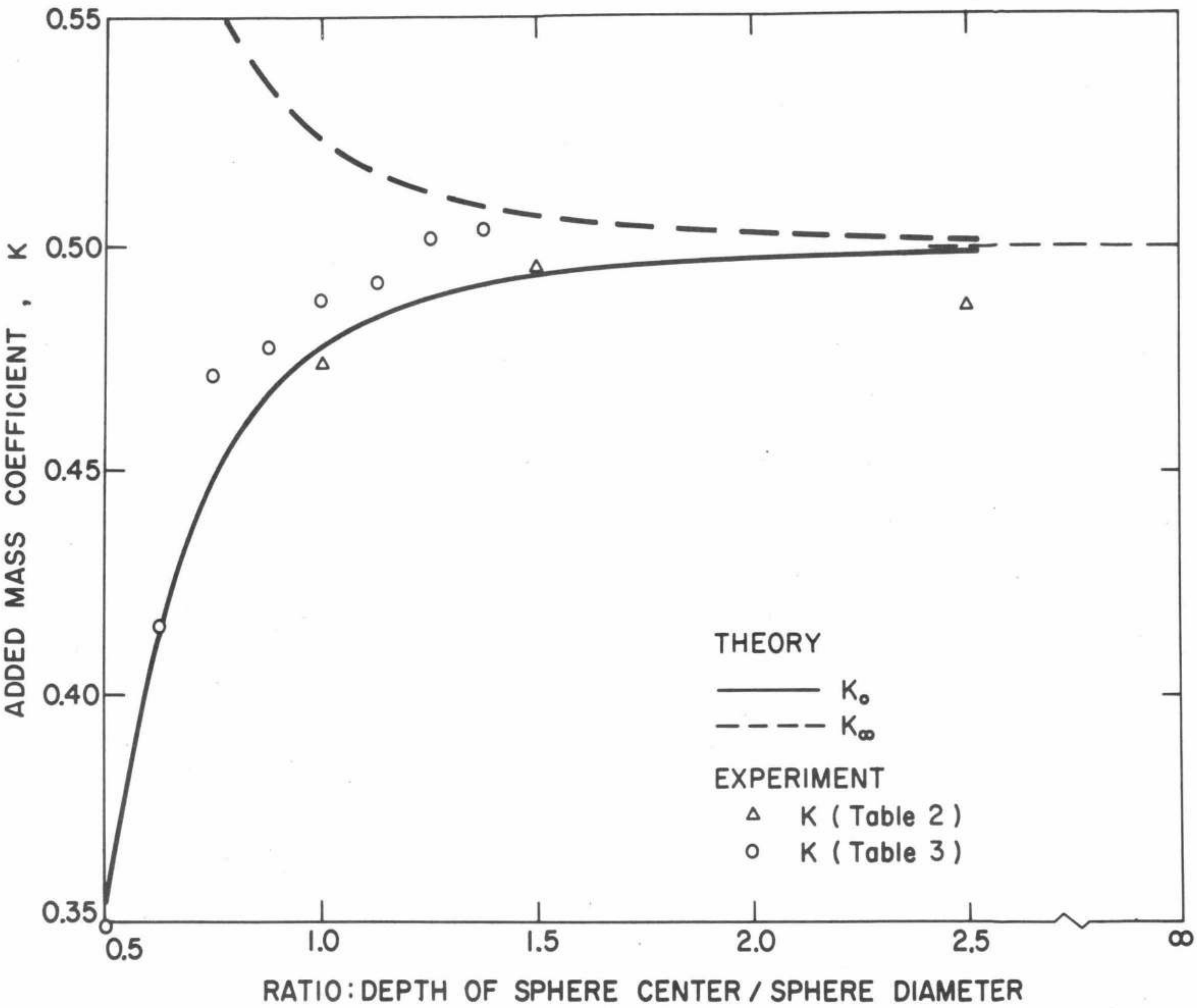

Figure 2 - Effect of Water Surface Proximity on the Added Mass of a 1-Inch Diameter Sphere Accelerated Vertically Upward from Rest

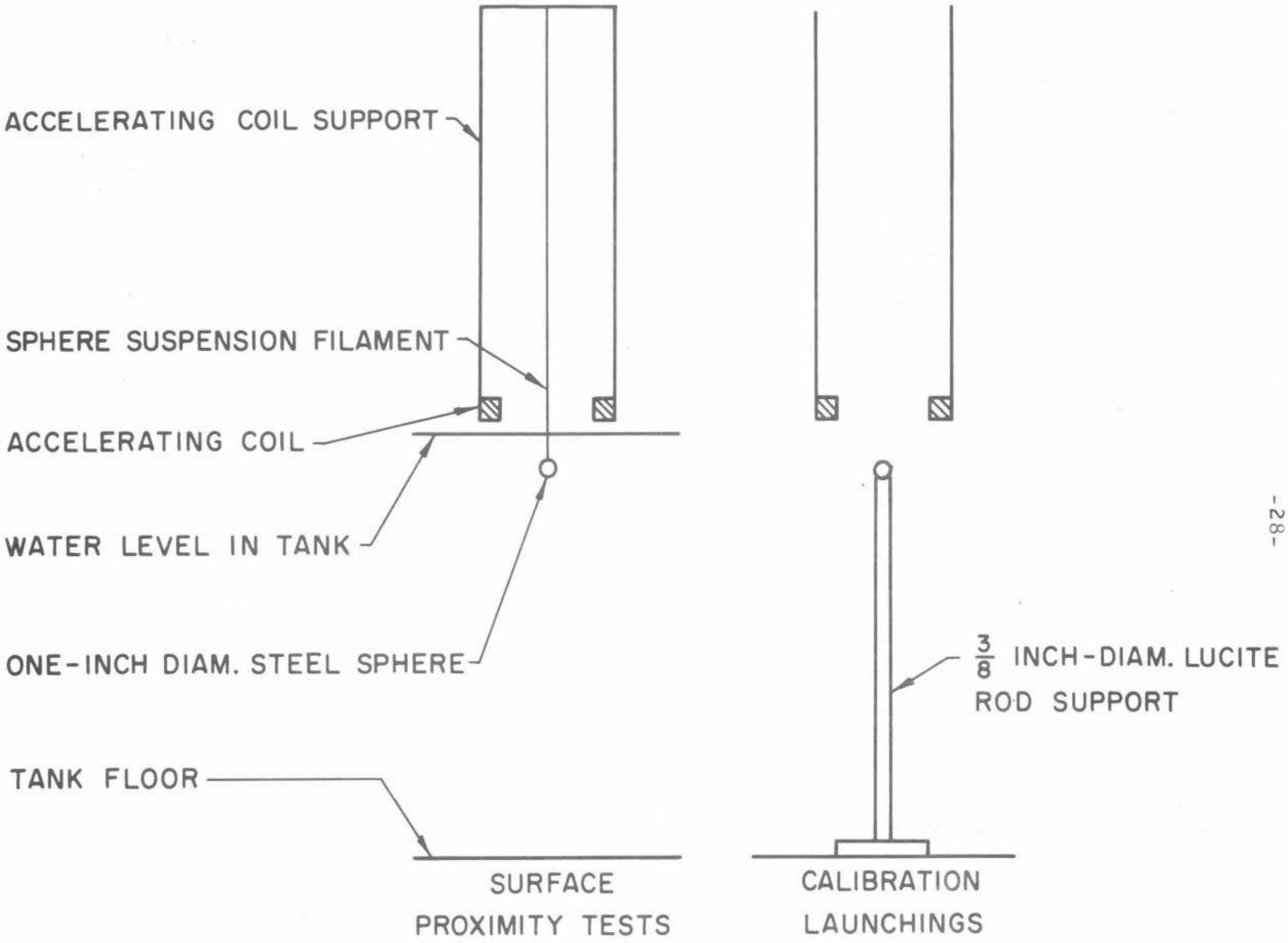

Figure 3 - Techniques Used to Accelerate Sphere Under Water and In Air

Appendix

Limit Points of Image Doublet Positions

It is of interest to determine the limit point of the primary sphere image doublet positions and hence the surface image doublet positions. For convenience, we assume positive values for the sphere doublet positions. It is obvious from their definition that the primary sphere doublet positions, h'_ν, must lie on the upper vertical radius of the primary sphere. From the recurrence relations, Eq. (35)

$$h'_o > h'_1 > h'_2 > \cdots > h'_\nu > h'_{\nu+1} > \cdots \tag{50}$$

and the h'_ν form a monotonically decreasing sequence. On the other hand, the point $h'_o - 1$ which lies on the upper vertical radius and circumference of the primary sphere is the greatest lower bound of points on the upper vertical radius and hence a lower bound of doublet positions. Since the doublet positions are bounded it follows from well-known limit theory that they must approach a limit. That is,

$$\lim_{\nu \to \infty} (h'_{\nu-1} - h'_\nu) = 0 , \qquad \lim_{\nu \to \infty} h'_{\nu-1} = h'_\nu \tag{51}$$

From the recurrence relations, Eq. (35) we obtain

$$h'_\nu h'_{\nu-1} = h'^2_o - 1 + h'_o (h'_{\nu-1} - h'_\nu) \tag{52}$$

Then in the limit as $\nu \longrightarrow \infty$

$$\lim_{\nu \to \infty} h'^2_\nu = h'^2_o - 1 \tag{53}$$

or

$$\lim_{v \to \infty} h_\nu' = (h_o'^2 - 1)^{\frac{1}{2}} \tag{54}$$

and $\sqrt{h_o'^2 - 1}$ is the greatest lower bound or limit point. To show that the limit point (and hence sphere image doublets) lies within the primary sphere doublet, it is sufficient to show that

$$(h_o'^2 - 1)^{\frac{1}{2}} \geq h_o' - 1 \tag{55}$$

Since $h_o' \geq 1$

$$h_o'^2 - 1 \geq h_o'^2 - 2h_o' + 1 = (h_o' - 1)^2 \tag{56}$$

and taking positive square roots, Eq. (55) follows.

The convergence of the doublet positions may also be established directly from the recurrence relations Eq. (35). From these the h_ν' can be shown as continuing fractions

$$h_\nu' = h_o' - \frac{1}{2h_o' -}\ \frac{1}{2h_o' -}\ \frac{1}{2h_o' -} \cdots \frac{1}{2h_o'} \tag{57}$$

to ν terms. From the theory of continued fractions (Ref. 8), the necessary and sufficient condition that h_ν' converges as $\nu \to \infty$ is that

$$\sum_{\nu=1}^{\infty} (2h_o')_\nu$$

diverges, which it obviously does since $h_o' \geq 1$. Hence h_ν' approaches a limit as $\nu \to \infty$, and since h_ν' decreases monotonically, it follows from limit theory that the limit is the greatest lower bound. The determination of the limit point follows, as shown above.

The limit point for surface image doublets is simply the reflection of the primary sphere image limit point in the surface. When the primary sphere is tangent to the fluid surface, both limit points coincide and lie on the surface point of tangency of the primary sphere doublet.

DISTRIBUTION LIST FOR

CALIFORNIA INSTITUTE OF TECHNOLOGY

REPORT E-124.2

CONTRACT N600(19)59368

NAVY	No. of Copies
Commander, Naval Ordnance Systems Command Department of the Navy Washington, D. C. 20360	
Attn: Code ORD-035	2
Code ORD-0523	1
Code ORD-05413	1
Code ORD-9132	2
Code NSP-001	1
Code ASW-2000	1
Commander, Naval Air Systems Command Department of the Navy Washington, D. C. 20360	
Attn: Code AIR-320	1
Commanding Officer and Director Naval Ship Research and Development Center Department of the Navy Washington, D. C. 20007	
Attn: Code 500	1
Commander Naval Missile Center Point Mugu, California 93041	
Attn: Technical Library	1
Commander Naval Weapon Center Inyokern, China Lake, California 93557	
Attn: Technical Library	1
Code 406	1
Commander Naval Undersea Warfare Center Pasadena Annex Pasadena, California 91107	
Attn: Code P-807	1
Code P-8552	1

NAVY (Continued)

	No. of Copies
Commander Naval Ordnance Laboratory White Oak, Silver Spring, Maryland 20910 Attn: Code 730	1
Code 530	1
Code 320	1
Commanding Officer Naval Underwater Weapons Research & Engineering Station Newport, Rhode Island 02844 Attn: Code RE	1
Commanding Officer and Director Naval Electronics Laboratory San Diego, California 92152	1
Commanding Officer Naval Torpedo Station Keyport, Washington 98345 Attn: J. Mason	1
Commander Naval Weapons Laboratory Dahlgren, Virginia 22448 Attn: Technical Library	1
Chief of Naval Research Department of the Navy Washington, D. C. 20360 Attn: Code 438	1
Code 416	1
Code 466	1
Commander, Naval Ships Systems Command Department of the Navy Washington, D. C. 20360 Attn: Code 2052	1
Code 034	1
Code 6136	1
Code 6114	1
Commander Naval Oceanographic Office Washington, D. C. 20390 Attn: Marine Science Department	1

NAVY (Continued)	No. of Copies
Superintendent U. S. Naval Postgraduate School Monterey, California 93940	1
Superintendent U. S. Naval Academy Annapolis, Maryland 21402	1
AIR FORCE	
Commander Office of Aerospace Research 1400 Wilson Boulevard Arlington, Virginia 22029	1
ARMY	
Commanding General, Army Material Command Department of the Army Washington, D. C. 20315 Attn: Chief Engineer	1
OTHER AGENCIES	
National Aeronautics and Space Administration Washington, D. C. 20546 Attn: Code UST	2
National Science Foundation Washington, D. C. 20550	1
Commander Defense Documentation Center Cameron Station Alexandria, Virginia 22314 Via: Commander, Naval Ordnance Systems Command Department of the Navy Washington, D. C. 20360 Attn: Code ORD-9132	16
EDUCATIONAL INSTITUTIONS	
Alden Hydraulic Laboratory Worcester Polytechnic Institute Worcester, Massachusetts 01609 Attn: L. J. Hooper	1

EDUCATIONAL INSTITUTIONS (Continued) | No. of Copies

Stevens Institute of Technology Castle Point Hoboken, New Jersey 07030 Attn: A. Suarez	1
Ordnance Research Laboratory Pennsylvania State University State College, Pennsylvania 16801 Attn: G. F. Wislicenus	1
Department of Naval Architecture & Marine Engineering Massachusetts Institute of Technology Cambridge, Massachusetts 02138 Attn: Library	1
Applied Physics Laboratory University of Washington Seattle, Washington 98105 Attn: Library	1

INDUSTRY

Douglas Aircraft Company, Inc. Aircraft Division 3855 Lakewood Boulevard Long Beach, California 90808 Attn: A. M. O. Smith	1
Eastern Research Group 120 Wall Street New York, New York 10005	1
General Dynamics Convair Division San Diego, California 92112	1
Grumman Aircraft Engineering Corporation Bethpage, Long Island, New York 11714 Attn: Research Department	1
Hydronautics, Inc. Pindell School Road Laurel, Maryland 20810 Attn: P. Eisenberg	
Ling-Temco-Vought Corporation P. O. Box 1508 Dallas, Texas 75221	1

INDUSTRY (Continued)	No. of Copies
Underwater Launch Department Lockheed Missile and Space Division Sunnyvale, California 94088	1

DOCUMENT CONTROL DATA - R&D

(Security classification of title, body of abstract and indexing annotation must be entered when the overall report is classified)

1. ORIGINATING ACTIVITY *(Corporate author)*

California Institute of Technology
Pasadena, California

2a. REPORT SECURITY CLASSIFICATION
UNCLASSIFIED

2b. GROUP

3. REPORT TITLE

Fluid Free Surface Proximity Effect on a Sphere Vertically Accelerated from Rest

4. DESCRIPTIVE NOTES *(Type of report and inclusive dates)*

Final Technical Report

5. AUTHOR(S) *(Last name, first name, initial)*

Waugh, John G. and Ellis, Albert T.

6. REPORT DATE
June 1967

7a. TOTAL NO. OF PAGES
33

7b. NO. OF REFS
8

8a. CONTRACT OR GRANT NO.
N600(19)59368

b. PROJECT NO. XXXXXX Task Assignment:
RRRE-04001/216-1/R009-01-01

c.

d.

9a. ORIGINATOR'S REPORT NUMBER(S)
E-124.2

9b. OTHER REPORT NO(S) *(Any other numbers that may be assigned this report)*

10. AVAILABILITY/LIMITATION NOTICES

11. SUPPLEMENTARY NOTES

12. SPONSORING MILITARY ACTIVITY
Naval Ordnance Systems Command
Weapon Dynamics Division
Department of the Navy

13. ABSTRACT

Theory is developed to estimate the effect of free surface proximity on the initial added mass of a sphere accelerated vertically upward from rest in an ideal fluid. It is assumed that the acceleration regime is sufficiently brief that inertial forces predominate and gravitational effects may be neglected. Results of tests in water indicate that while there are slight viscous and gravitational effects over the acceleration regime, the agreement between theory and experiment is good. It is concluded that over briefer acceleration regimes these effects would decrease and the agreement would improve.

14. KEY WORD	LINK A		LINK B		LINK C	
	ROLE	WT	ROLE	WT	ROLE	WT
Added Mass Free Surface Effect Ideal Fluid Theory Real Fluid Effects						

INSTRUCTIONS

1. ORIGINATING ACTIVITY: Enter the name and address of the contractor, subcontractor, grantee, Department of Defense activity or other organization *(corporate author)* issuing the report.

2*a*. REPORT SECURITY CLASSIFICATION: Enter the overall security classification of the report. Indicate whether "Restricted Data" is included. Marking is to be in accordance with appropriate security regulations.

2*b*. GROUP: Automatic downgrading is specified in DoD Directive 5200.10 and Armed Forces Industrial Manual. Enter the group number. Also, when applicable, show that optional markings have been used for Group 3 and Group 4 as authorized.

3. REPORT TITLE: Enter the complete report title in all capital letters. Titles in all cases should be unclassified. If a meaningful title cannot be selected without classification, show title classification in all capitals in parenthesis immediately following the title.

4. DESCRIPTIVE NOTES: If appropriate, enter the type of report, e.g., interim, progress, summary, annual, or final. Give the inclusive dates when a specific reporting period is covered.

5. AUTHOR(S): Enter the name(s) of author(s) as shown on or in the report. Enter last name, first name, middle initial. If military, show rank and branch of service. The name of the principal author is an absolute minimum requirement.

6. REPORT DATE: Enter the date of the report as day, month, year, or month, year. If more than one date appears on the report, use date of publication.

7*a*. TOTAL NUMBER OF PAGES: The total page count should follow normal pagination procedures, i.e., enter the number of pages containing information.

7*b*. NUMBER OF REFERENCES: Enter the total number of references cited in the report.

8*a*. CONTRACT OR GRANT NUMBER: If appropriate, enter the applicable number of the contract or grant under which the report was written.

8*b*, 8*c*, & 8*d*. PROJECT NUMBER: Enter the appropriate military department identification, such as project number, subproject number, system numbers, task number, etc.

9*a*. ORIGINATOR'S REPORT NUMBER(S): Enter the official report number by which the document will be identified and controlled by the originating activity. This number must be unique to this report.

9*b*. OTHER REPORT NUMBER(S): If the report has been assigned any other report numbers *(either by the originator or by the sponsor)*, also enter this number(s).

10. AVAILABILITY/LIMITATION NOTICES: Enter any limitations on further dissemination of the report, other than those imposed by security classification, using standard statements such as:

(1) "Qualified requesters may obtain copies of this report from DDC."

(2) "Foreign announcement and dissemination of this report by DDC is not authorized."

(3) "U. S. Government agencies may obtain copies of this report directly from DDC. Other qualified DDC users shall request through
____."

(4) "U. S. military agencies may obtain copies of this report directly from DDC. Other qualified users shall request through
____."

(5) "All distribution of this report is controlled. Qualified DDC users shall request through
____."

If the report has been furnished to the Office of Technical Services, Department of Commerce, for sale to the public, indicate this fact and enter the price, if known.

11. SUPPLEMENTARY NOTES: Use for additional explanatory notes.

12. SPONSORING MILITARY ACTIVITY: Enter the name of the departmental project office or laboratory sponsoring *(paying for)* the research and development. Include address.

13. ABSTRACT: Enter an abstract giving a brief and factual summary of the document indicative of the report, even though it may also appear elsewhere in the body of the technical report. If additional space is required, a continuation sheet shall be attached.

It is highly desirable that the abstract of classified reports be unclassified. Each paragraph of the abstract shall end with an indication of the military security classification of the information in the paragraph, represented as *(TS)*, *(S)*, *(C)*, or *(U)*.

There is no limitation on the length of the abstract. However, the suggested length is from 150 to 225 words.

14. KEY WORDS: Key words are technically meaningful terms or short phrases that characterize a report and may be used as index entries for cataloging the report. Key words must be selected so that no security classification is required. Identifiers, such as equipment model designation, trade name, military project code name, geographic location, may be used as key words but will be followed by an indication of technical context. The assignment of links, roles, and weights is optional.